PROCEEDINGS OF SCIENCE

Latest results from the Pierre Auger Observatory

Esteban Roulet*, **for the Pierre Auger Collaboration** †
CONICET, Centro Atómico Bariloche
Bustillo 9500, Bariloche, 8400, Argentina
E-mail: roulet@cab.cnea.gov.ar

Recent results obtained with the Pierre Auger Observatory are described. These include measurements of the spectrum, anisotropies and composition of ultra-high energy cosmic rays. The ankle of the spectrum is measured at 4×10^{18} eV and a suppression above 3×10^{19} eV consistent with the GZK effect is observed. At energies above 5.5×10^{19} eV a correlation with the distribution of nearby extragalactic objects is found, including an excess around the direction of Centaurus A, the nearest radio loud active galaxy. Measurements of the depth of shower maximum and its fluctuations suggest a gradual change in the average mass of the primary cosmic rays (under standard extrapolations of hadronic interaction models), being the results consistent with a light composition consisting mostly of protons at few$\times10^{18}$ eV and approaching the expectations from iron nuclei at 4×10^{19} eV. Upper bounds on the photon fraction and the neutrino fluxes are also obtained.

Quarks, Strings and the Cosmos - Héctor Rubinstein Memorial Symposium
August 09-11, 2010
AlbaNova, Stockholm, Sweden

*Speaker.

†Full author list available in http://www.auger.org/archive/authors_2010_11.html. Work partially supported by ANPCyT PICT 1334 and by CONICET PIP 01830. Dedicated to the memory of Héctor Rubinstein and his passion for the physics of astroparticles.

PoS(HRMS)034

1. Introduction

The Pierre Auger Observatory, built near the town of Malargüe in Argentina, has been gathering data since January 2004 [1]. It reached its baseline design covering 3000 km^2 with 1600 water Cherenkov detectors overlooked by 24 fluorescence telescopes by mid 2008 and by the end of 2009 had accumulated a total exposure of about twenty thousand km^2 sr yr, much larger than that of all previous air shower experiments combined. The surface detector has a duty cycle of almost 100 %, collecting then the vast majority of the data which are used for spectrum measurements and anisotropy searches. On the other hand, simultaneous observations with both the fluorescence and surface detectors are possible for $\sim 15\%$ of the events (those observed during moonless nights with no clouds), for which the longitudinal development in the atmosphere as well as the lateral profile on the ground can be measured. This allows the cross calibration between the two detection techniques, since the UV fluorescent light emitted by the nitrogen molecules excited by the electromagnetic component of the air shower provide an almost calorimetric measurement of the energy of the primaries. It also allows to determine the depth of maximum development of the shower, which encodes precious information on the composition of the primaries and the properties of the first hadronic interactions. The studies of the cosmic rays at the highest energies with the Auger Observatory has already allowed to start addressing many of the old questions that motivated its construction by measuring the features present in the spectrum, searching for anisotropies in the cosmic ray arrival directions distribution or constraining the composition of the primary cosmic rays.

2. Spectrum

In order to determine the cosmic ray spectrum, a reliable estimate of the exposure is necessary, and hence a strict event selection is performed requiring that the detector with the largest signal be surrounded by a full hexagon of working detectors (for high energy anisotropy searches instead, a relaxed trigger requires only 5 active detectors around the 'hottest' one and that the shower core be contained in an active triangle). Events with zenith angles below 60° are used in the following studies and in this case the surface array is fully efficient only above 3 EeV (where 1 EeV $\equiv 10^{18}$ eV), in which case all showers trigger at least three detectors and can hence be reconstructed. Below this energy the surface detector efficiency becomes less certain (depending in particular on the composition of the cosmic rays), so that the spectrum is obtained instead using hybrid events. The resulting measured spectrum [2] above 1 EeV is shown in Fig. 1. A piece wise fit using power laws ($\mathrm{d}N/\mathrm{d}E \propto E^{-\alpha}$) shows that there are two clear transitions at 4.1 EeV and 29 EeV. The first feature is the so-called ankle, in which the spectral index changes from $\alpha = 3.26 \pm 0.04$ to 2.59 ± 0.02, and the second feature involves a transition to a much steeper spectrum (the power law fit leading to $\alpha = 4.3 \pm 0.2$), with the spectrum falling to half the value that would be obtained from an extrapolation of the lower energy fit at $E_{1/2} \simeq 40$ EeV. One has to keep in mind that systematic effects on the energy determination amount to 22%, and are hence significant. In particular, the different normalization of the spectrum measured by the HiRes experiment, also shown for comparison in fig. 1, is most likely due to a systematic energy mismatch between the two experiments.

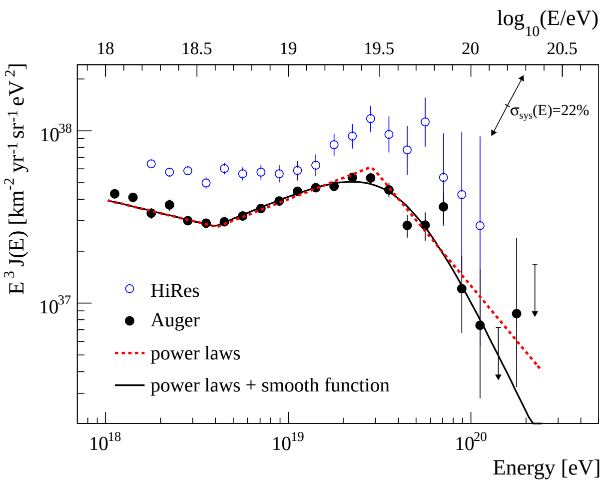

Figure 1: Spectrum measured above 1 EeV (solid dots) and power law fits with breaks (dotted line). For comparison also the HiRes measurements are displayed (open dots).

The physical origin of the ankle is still uncertain, being the main candidate scenarios to explain this feature those relating it to the transition from a dying galactic component to a harder extragalactic component becoming dominant, or alternatively the so-called dip-scenario [3], in which cosmic rays are assumed to be extragalactic protons down to energies below 1 EeV and the concave shape observed arises from the effect of energy losses by pair creation with cosmic microwave background (CMB) photons. To properly fit the observed spectral shape this last scenario requires soft spectra at the sources (α at the source being typically $\alpha_g \simeq$ 2.4-2.7) and/or strong evolution of the sources with redshift, what makes the distant sources intrinsically brighter (or more abundant) so that a larger fraction of the observed protons come from far away and are hence more affected by interactions with CMB photons. Also an upward shift of the energy scale of Auger by $\sim$ 40% would be required in this scenario to fit the location of the dip in the spectrum.

Anisotropy measurements will help to distinguish among the two scenarios, because the galactic/extragalactic transition may lead to measurable dipole type patterns in the arrival direction distribution resulting from the diffusive escape of the galactic cosmic rays, and already significant constraints have been obtained by Auger at EeV energies [4]. Also composition measurements are important because galactic cosmic rays at EeV energies are expected to be dominated by heavy nuclei, since their confinement by galactic magnetic fields is a rigidity dependent effect. Enhancements of the Auger observatory to improve the sensitivity down to energies of 10^{17} eV, such as the HEAT fluorescence detectors or the AMIGA infill and muon detectors, will help to shed light on these issues in the near future.

The second feature mentioned, i.e. the suppression observed at the highest energies, is similar to the expectations from the so called GZK effect associated to the attenuation of extragalactic protons by photo-pion production off CMB photons (this suppression was predicted by Greisen and Zatsepin and Kuz'min just after the discovery of the CMB). Also the photodisintegration of nuclei as heavy as iron would lead to similar features, while lighter nuclei would instead show a suppression down to a lower energy threshold, in approximate proportion to their masses. Note that a change in the injection spectrum at the sources may also contribute in part to the observed

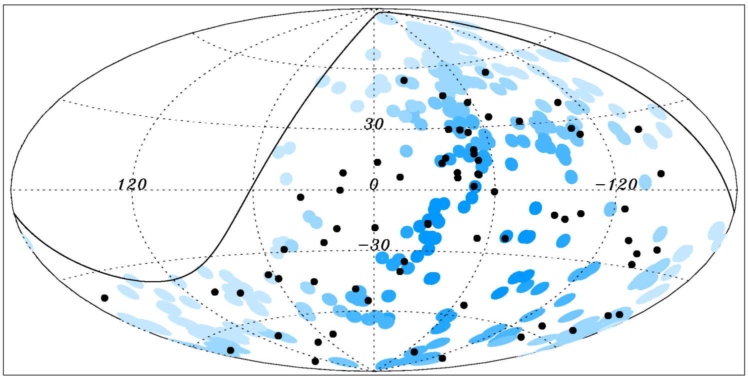

Figure 2: Arrival directions of the events above 55 EeV (dots) and 3.1° circles around the directions towards AGN in the VCV catalog closer than 75 Mpc.

spectral shape.

3. Anisotropies

Searches for localized anisotropies are motivated by the fact that cosmic ray trajectories in galactic and extragalactic magnetic fields become straighter as the energy increases, being for instance the typical deflection for a nucleus of charge Z traveling a distance L in the galactic field (for which the regular component has a strength of $\sim 3\ \mu$G coherent over scales $\sim$ kpc) of

$$\delta \simeq 3^\circ Z \left(\frac{B}{3\ \mu\mathrm{G}}\right)\left(\frac{L}{\mathrm{kpc}}\right)\left(\frac{60\ \mathrm{EeV}}{E}\right). \tag{3.1}$$

This gives then the hope that cosmic ray astronomy may become feasible at ultra-high energies. On the other hand, since above the GZK threshold the energies of extragalactic cosmic rays are significantly attenuated as they propagate through the cosmic photon backgrounds, setting a sufficiently high energy threshold implies that only sources within a relatively close-by neighborhood can contribute to the fluxes observed at Earth. For instance, for a uniform distribution of proton sources 90% of the cosmic rays reaching the Earth with energies above 60 EeV should have been produced within about 200 Mpc [5], and comparable 'GZK horizons' are also found in the case of Fe sources. Then, an efficient way to search for an anisotropy pattern, before any individual source clearly stands up above the background, is to look for a correlation within a certain angular window between the arrival directions of the events above a certain threshold energy and the location of a certain type of candidate sources within a given distance.

One class of potential source population that may be able to accelerate particles up to these extreme energies is the Active Galactic Nuclei (AGN), consisting of the supermassive black holes (with masses up to $\sim 10^9 M_\odot$) accreting matter in the center of galaxies and emitting powerful jets. An analysis performed by the Auger Collaboration [6, 7] indeed established a correlation with the AGN in the Véron Cetty and Véron (VCV) catalog (which is actually a compilation of catalogs). This correlation was most significant for events above 55 EeV and angular separations of less than 3.1° from AGN closer than 75 Mpc. In the latest study with data up to the end of 2009, the fraction of events correlating within those parameters (excluding the events from the initial period used to

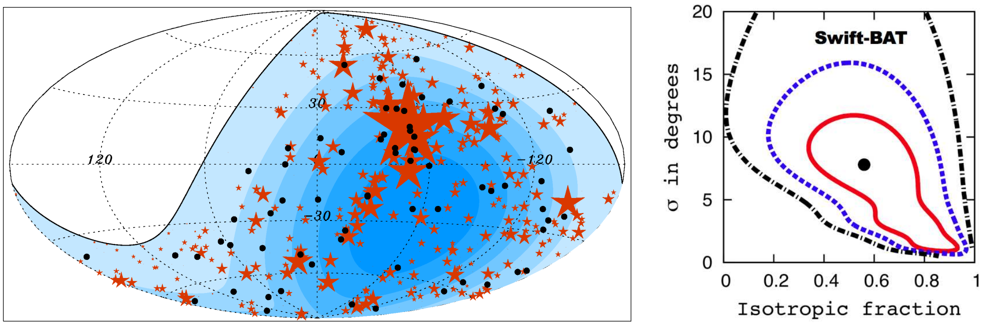

Figure 3: Left panel: map of arrival directions of the events above 55 EeV and AGNs observed in X-rays by SWIFT. Right panel: Likelihood contours (1, 2 and 3 σ) vs. the isotropic fraction and the smoothing angular scale σ.

fix those values) is 38^{+7}_{-6}%, well above the 21% that would be expected if the distribution were isotropic [8]. A map of the observed arrival directions (dots) in galactic coordinates is shown in fig. 2, displaying also circles of 3.1° radius around the location of nearby VCV AGN. One finds that 29 out of the 69 events do indeed fall inside one of the circles. Note that due to obscuration effects the catalogs are particularly incomplete near the galactic plane, and hence it is understandable that most of the events within 10° of the galactic plane do not correlate with objects in the catalog.

Alternative studies with different catalogs were also performed. For instance, figure 3 (left panel) displays the same events and the distribution of nearby (within 200 Mpc) AGN observed in X-rays by the SWIFT satellite. The size of the stars in the plot is proportional to the measured X-ray fluxes, to a weight proportional to the attenuation expected due to the GZK effect and to the relative exposure of the observatory in that direction. Smoothing out the sources in this map with gaussian windows of a given angular scale, and adding a certain fraction f_{iso} of isotropic background, a likelihood test leads to optimal parameters (displayed in the right panel) corresponding to angular scales below $\sim 10°$ and isotropic fractions between 40 and 80%. It is clear that a model consisting of only the sources in the catalog with deflections of a few degrees would not be consistent with the data. The isotropic fraction that is required could well be accounting for the faint or faraway sources not included in the catalog, or for the contribution from a strongly deflected heavy cosmic ray component. We note that the actual sources of cosmic rays may be different than the AGN (e.g. they could be gamma ray bursts, galaxy clusters or colliding galaxies), and hence in the studies described the AGN may just be acting as a tracer of a different but similarly distributed population. Also the angular scales inferred are only indicative and may not reflect the actual deflection suffered by cosmic rays, since the closest AGN to an event need not be its source.

It is important that the correlation with nearby extragalactic objects observed is consistent with cosmic rays from more distant sources having lost energy in accordance with the flux suppression seen in the energy spectrum, and hence this further supports the interpretation that this suppression is related to the GZK effect and not just due to the exhaustion of the sources.

A significant concentration of events is found around the location of Centaurus A (corresponding to the largest star in the left panel of fig. 3), which is particularly interesting because this AGN lies at only ~ 4 Mpc from us. Figure 4 shows the number of observed events as a function of the angular distance from Cen A together with the isotropic expectations (average and 68, 95 and

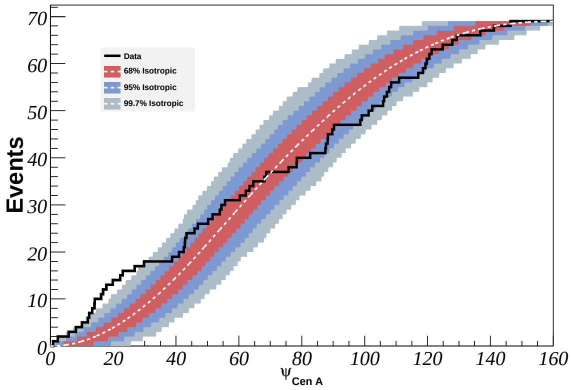

Figure 4: Cumulative number of events vs. the angular distance from Centaurus A, compared to the isotropic expectation.

99.7% expected isotropic dispersion). The most significant departure from isotropy is seen for 18°, for which 13 events are observed while only 3 are expected. Whether these events come from Cen A or from other sources, such as from the Centaurus cluster lying behind (at $\sim$ 45 Mpc) is still unclear, but this is certainly a region that looks specially promising for future anisotropy searches.

4. Composition

The other important piece of information one would like to know about the cosmic rays is their composition, i.e. whether they are protons or heavier nuclei and if there are some detectable fluxes of photons or neutrinos. This knowledge could also help to better understand the origin of the different features in the spectrum and the properties of the acceleration and propagation processes.

Purely electromagnetic showers, like those initiated by photons, develop by a combination of $e^{\pm}$ pair production processes by photons and of electron (or positron) bremsstrahlung, so that after each interaction length the number of particles in the shower essentially doubles. Hence, the total number of particles grows exponentially with the grammage traversed, until the energies of the individual particles fall below a critical value $E_c \simeq 86$ MeV for which the $e^{\pm}$ energy losses by ionization become important and the shower begins to attenuate. At the maximum of the shower the number of particles is then $N_{max} \simeq E/E_c \simeq 10^{11} E/\text{EeV}$ and the depth of shower maximum X_{max} depends logarithmically on the energy of the primary (note that the radiation length in air is $X_0 = 37$ g/cm^2, and the interaction length is $\lambda \simeq X_0 \ln 2$, so that there are typically 30-40 interaction lengths before the ultra-high energy photon shower reaches the maximum).

Hadronic showers develop differently because in the interaction of a proton with a nucleus in the air a very large number, of order $\sim 10^2$ at the highest energies, of secondaries are produced. These secondaries are mostly pions, and the neutral ones (amounting to about 1/3 of the total) immediately decay into two photons and feed the electromagnetic component of the shower, while the charged ones will reinteract hadronically producing again a large number of pions. This process repeats typically for $n \simeq 5$ or 6 times until the individual pion energies are below a few tens of GeV and the charged pions are able to decay before reinteracting, producing in this way muons

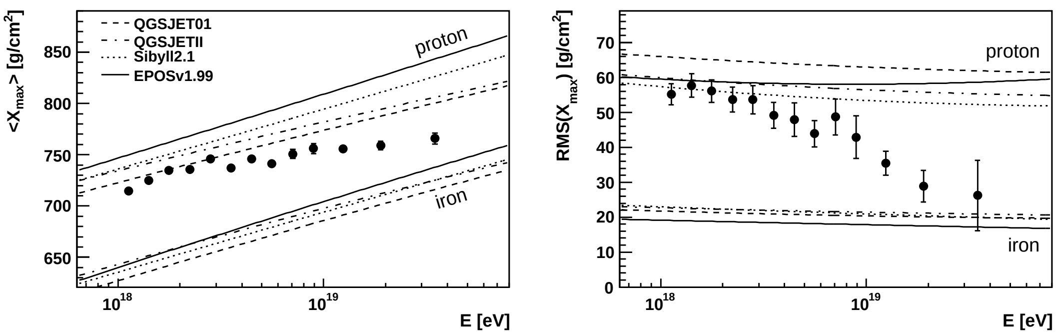

Figure 5: Measured values of X_{max} (left) and its RMS (right) as a function of energy.

and neutrinos, which carry away a fraction $(2/3)^n \simeq 10\%$ of the primary energy. The remaining $\sim 90\%$ is what went into the electromagnetic component through the neutral pions of the different generations. Since the multiplication of particles in an hadronic shower proceeds at a faster rate than in the case of photon primaries, the maximum of the shower is reached earlier. The other distinguishing signature of hadronic showers is the presence of a sizeable number of muons reaching the ground. In the case of primary nuclei, a simple description can be obtained with the so-called superposition model, which considers the shower produced by a nucleus of mass number A and energy E as being a collection of A showers produced by nucleons of energy E/A. The resulting shower will then develop earlier (since the depth of maximum of a proton shower scales as $\log E$) and will also have smaller fluctuations, since the individual maxima of the A subshowers get averaged out. These two observables (X_{max} and its fluctuations) allow then to get information on the cosmic ray composition. The results of the measurements performed with the Auger fluorescence detectors [9] are displayed in figure 5, together with the predictions for proton and Fe primaries obtained using different hadronic interaction models, which actually need to be extrapolated to energies well beyond those measured at accelerators, and are hence still affected by significant uncertainties. A transition from a light composition at few EeV towards one approaching the expectations from heavier nuclei (even close to those of iron) at ~ 40 EeV is observed. One has to keep in mind that an increase in the proton nucleus cross section beyond what is considered in the usually adopted hadronic models would also affect the inferred nuclear masses since in this case protons could mimic the expected behavior of heavier nuclei.

The values of X_{max} shown in figure 5 also indicate that the fraction of showers that could be produced by photons is small, since those would be deeply penetrating and hence lead to X_{max} values larger than the predictions for protons. Moreover, a more restrictive constraint on the photon fraction can be obtained using the larger statistics of the surface detector and exploiting the fact that purely electromagnetic showers, having no muonic component, lead to slower rise-times of the signals in the water Cherenkov detectors, and also developing deeper in the atmosphere they lead to shower fronts with smaller radius of curvature. The results of these two measurements [10] allow then to set the bounds on the photon fraction displayed in figure 6, which for instance exclude photon fractions larger than 2% for $E > 10$ EeV. These bounds already exclude many ‘top-down’ models for the production of ultra-high energy cosmic rays through decays of super heavy particles or topological defects, since these would lead to significant photon fluxes (some predictions are

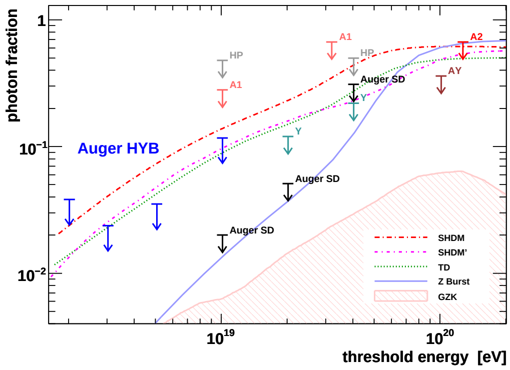

Figure 6: Bounds on the allowed fraction of photons vs. the energy threshold.

shown in the figure), and hence the standard scenarios of 'bottom-up' acceleration in astrophysical sources is reinforced. The present sensitivity is still insufficient to detect the photons that could be produced if ultra-high energy cosmic rays are extragalactic protons that get attenuated by photo-pion interactions with the CMB. The neutral pion decays would lead to photon fluxes somewhere in the shaded region of the plot, which will start to be tested in a few years with the continuous operation of the Auger Observatory.

Another important search is that for diffuse neutrino fluxes [11], such as those expected to result from the decays of the charged pions produced in the attenuation of extragalactic protons (cosmogenic neutrinos). Being weakly interacting, the neutrinos arriving near the vertical have a small chance to interact in the atmosphere, but on the other hand, neutrinos arriving near the horizon may have a first interaction not far from the detector, and hence produce horizontal showers that are young (i.e. with significant electromagnetic component), unlike the horizontal showers produced by hadrons that start very far away at the top of the atmosphere and hence have their electromagnetic component completely attenuated and lead only to very narrow pulses in the detectors due to the surviving muon component. Another effective way to observe neutrino induced showers is by looking at those produced by tau neutrinos coming from slightly below the horizon. In this case, a charged current interaction in the rock produces a tau lepton that can travel several km and eventually exit the ground and decay above the detector, producing an observable shower. Since neutrino oscillations are expected to lead to an equal admixture of the different flavors, even in the case that the sources produce only muon and electron neutrinos by pion decays, tau neutrino fluxes are also expected. These searches for upgoing showers represent actually the most sensitive way to look for diffuse neutrinos with the Auger Observatory. The resulting bounds are displayed in figure 7. They are particularly sensitive at EeV energies, which is just the energy range were cosmogenic neutrinos are expected to peak. However, the present sensitivity is still above the most optimistic predictions (shaded region in the plot) but some improvements are expected to be obtained with increased statistics. Observation of these diffuse neutrino fluxes would strongly favor a proton composition at the highest energies, because heavy nuclei lead to much smaller expected neutrino fluxes since having smaller speeds they are below the threshold for pion production until much higher energies.

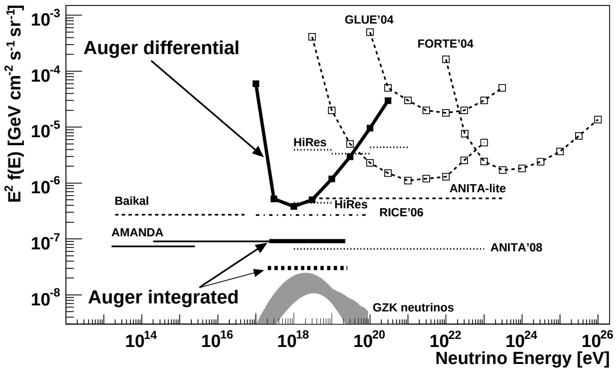

Figure 7: Neutrino bounds

References

[1] The Pierre Auger Collaboration, Nucl. Instr. and Methods in Physics Research A613 (2010), 29-39.

[2] The Pierre Auger Collaboration, Phys. Lett. B 685 (2010) 239.

[3] V. S. Berezinsky and S. I. Grigorieva, Astron. and Astrophys. 199 (1988) 1.

[4] R. Bonino, for the Pierre Auger Collaboration, ICRC 2009, arXiv:0906.2347.

[5] D. Harari, S. Mollerach and E. Roulet, JCAP 0611:012 (2006).

[6] The Pierre Auger Collaboration, Science 318 (2007) 938.

[7] The Pierre Auger Collaboration, Astropart. Phys. 29 (2008) 188.

[8] The Pierre Auger Collaboration, Astroparticle Physics 34 (2010) 314.

[9] The Pierre Auger Collaboration, Phys. Rev. Lett. 104 (2010) 091101.

[10] The Pierre Auger Collaboration, Astropart. Phys. 29 (2008) 243; Astropart. Phys. 31 (2009) 399.

[11] The Pierre Auger Collaboration, Phys. Rev. Lett. 100 (2008) 211101; Phys. Rev. D79 (2009) 102001.